The
Allied
Corporation

Bendix
Guidance
Systems
Division

Teterboro
New Jersey 07608

ADAPTIVE MOMENTUM MANAGEMENT FOR LARGE SPACE STRUCTURES

Final Report
31 January 1987

Prepared For:

George C. Marshall
Space Flight Center -
Huntsville, Alabama

NASA Contract no.
NAS8-36488
Exhibit D

May 1, 1986
to
January 31 1987

PREPARED BY

E. Hahn
Technical Manager

Table of Contents

Section No.	Description	Page
	Foreword	i
	List of Illustrations	ii
	Abstract	1
	Nomenclature	2
1.0	Introduction	7
2.0	Development of Concepts	11
3.0	Development of Simulation Without Dynamics	13
4.0	Momentum Management Control Laws	15
5.0	Simulation results Without Dynamics	21
6.0	Verification of results with dynamics	30
7.0	Conclusions	36
8.0	Summary	38
9.0	References	39

List of Illustrations

Figure No.	Description	Page
1	Dual Keel in IOC Configuration.....	9
2	Reference Coordinate Systems.....	12
3	Momentum Management Simulation without Dynamics.....	13
4	Momentum Management Block Diagram.....	20
5	POP Axis Momentum Management Response.....	22
6	POP Axis Response for First 2 Orbits.....	23
7	POP Response with Incorrect Inertia Estimate.....	24
8	POP Response with Incorrect Inertia Estimate and Adaptive Update Scheme.....	25
9	IOP Axes Momentum Management Response.....	26
10	IOP Axes Aerodynamic Torque Induced Momentum.....	27
11	IOP Momentum Management with Initial Accumulated IOP Momentum.....	28
12	IOP Axes Resporse for First 2 Orbits.....	29
13	Simulation with Vehicle Dynamics.....	32
14	Simulation with Vehicle Dynamics, 6 DGCMGs and Kennel Steering law.....	33
15	Typical Inner Gimbal Rate Profile during Active Orbit.....	34
16	Typical Outer Gimbal Rate Profile during Active Orbit.....	35

Foreword

This final report is submitted in accordance with "Scope of Work,Exhibit D" for contract NAS8-36488. This study was directed from Bendix Guidance Systems Division(GSD), Allied Coroporation. Mr Eric Hahn was Study Manager and he appreciates the valuable guidance of Ms. Miriam Hopkins of the Marshall Space Flight Center (MSFC) who was the contracting officer representative. Additional important suggestions were made by Mr. Harry Buchanan and Mr. Stan Carroll of MSFC and Mr. Ray Kaczynski of Bendix GSD.

Abstract

The report discusses momentum management for a Large Space Structure(LSS) with the structure selected configuration being the Initial Orbital Configuration(IOC) of the dual keel space station. The external torques considered were gravity gradient and aerodynamic torques. The goal of the momentum management scheme developed is to remove the bias components of the external torques and center the cyclic components of the stored angular momentum. The scheme investigated is adaptive to uncertainties of the inertia tensor and requires only approximate knowledge of principal moments of inertia. Computational requirements are minimal and should present no implementation problem in a flight type computer and the method proposed is shown to be effective in the presence of attitude control bandwidths as low as .01 radian/sec.

Nomenclature

CDG	Control Design Group
CMG	Control Moment Gyro
DGCMG	Double Gimbal Control Moment Gyro
$dq_{lv/v}$	4x1 non-normalized quaternion representing vehicle attitude change with respect to LV during last computation cycle
G_h	Total gain, including GG constant, inertia estimate and sample time, to remove momentum error
G_θ	Total gain, including GG constant and inertia estimate, to remove sampled bias torque
Deg	Degree
Ft	Foot
GG	Gravity gradient
GSD	Guidance System Division
$\bar{H}_{bias}$	3x1 vector of bias momentum in vehicle space
$\bar{H}_{cmg}$	3x1 vector of CMG momentum in vehicle space
$\bar{H}_{cmg(oi)}$	3x1 vector of CMG momentum in inertial space
$\bar{H}_i$	Momentum of i-th CMG used in steering law

Nomenclature (Continued)

$H_{(n-1)x}, H_{(n-1)y}$	X,Y-axes resp. momentum error at previous sample
H_{nx}, H_{ny}	Current X,Y-axes resp. momentum error
$H_{(n+1)x}, H_{(n+1)y}$	Expected X,Y-axes resp. momentum error at next sample
$\bar{H}_t$	3x1 vector of total momentum in vehicle space
$\bar{H}_{t(oi)}$	3x1 vector of total momentum(vehicle + CMG)
$\bar{H}_v$	3x1 vector of vehicle momentum in vehicle space
$\bar{H}_{v(oi)}$	3x1 vector of vehicle momentum in inertial space
Hz	Hertz
H_{zavg}	Average value of Z-axis CMG momentum used to compensate effect of gyroscopic torque in X-axis GG bias torque extraction algorithm
IOC	Initial Orbital Configuration
IOP	In orbit plane
I_v	3x3 tensor of vehicle inertia in vehicle frame
K_h	Normalized gain to remove momentum error
K_θ	Normalized gain to remove sampled bias torque
I_{xp}	Vehicle X-axis principal inertia
I_{yp}	Vehicle Y-axis principal inertia

Nomenclature (Continued)

K_p	Proportional gain used in vehicle control law
K_r	Integral gain used in vehicle control law
Lb	Pound
LSS	Large Space Structure
M	Meter
MSFC	Marshall Space Flight Center
N	Newton
POP	Perpendicular to orbit plane
RCS	Reaction Control System
sec	Second
$q_{lv/v}$	4x1 normalized quaternion representing vehicle attitude with respect to LV
$q^{+}_{lv/v}$	4x1 normalized updated quaternion representing vehicle attitude with respect to LV
$q_{oi/lv}$	4x1 quaternion representing LV with respect to inertial space
$Q_{v/lv}$	4x4 equivalent quaternion form representing LV with respect to vehicle
$q_{v/oi}$	4x1 quaternion representing orbit inertial with respect to vehicle

Nomenclature (Continued)

$\bar{T}_{aero}$	3x1 vector of aerodynamic torque in vehicle space
$\bar{T}_{cmd}$	3x1 vector of vehicle torque command from control law
$\bar{T}_{i}$	3x1 vector external torque(GG & Aero) in vehicle space
$\bar{T}_{d(oi)}$	3x1 external torque in inertial space
$\bar{T}_{gy}$	3x1 vector of gyroscopic torque in vehicle space
T_m	Momentum management sample time
$T_{oi/v}$	3x3 transformation matrix from inertial to vehicle space
$T_{v/oi}$	3x3 transformation matrix from vehicle to inertial space
α_i	Inner gimbal angle of i-th CMG
$\dot{\alpha}_i$	Inner gimbal rate of i-th CMG
β_i	Outer gimbal angle of i-th CMG
$\dot{\beta}_i$	Outer gimbal rate of i-th CMG
Δt	Simulation time increment
$\Delta I_x, \Delta I_y$	X,Y-axes resp. inertia differences
$\Delta I_{x(est)}, \Delta I_{y(est)}$	X,Y-axes resp. estimated inertia differences
θ_{xc}	X-axis maneuver angle command

Nomenclature (Continued)

$\dot{\theta}_{xp}$	X-axis previous angular rate command
θ_{yc}	Y-axis maneuver angle command
$\dot{\theta}_{yh}$	Y-axis rate commanded to remove accumulated momentum
$\dot{\theta}_{yp}$	Y-axis previous angular rate command
$\bar{\omega}_c$	3x1 vector of total vehicle rate command
$\dot{\bar{\omega}}_{cmd}$	3x1 vector of vehicle acceleration command
$\bar{\omega}_{lv/v}$	3x1 vector of vehicle rate command from momentum management control law
$\bar{\omega}_0$	3x1 vector of orbital rate in LV frame$(0, -\omega_0, 0)$
$\bar{\omega}_{0(v)}$	3x1 vector of orbital rate in vehicle frame
$\bar{\omega}_v$	3x1 vector of total vehicle rate

1.0 Introduction

Two types of missions for an LSS are often considered: Local vertical(LV) and Inertial. Neglecting other considerations, each type of vehicle presents challenges in the implementation of momentum management. For an inertial vehicle, if the principal axes are rotated out of the orbit plane about an axis in the orbit plane, a gravity gradient(GG) bias torque will exist in the orbit plane. Additionally, even if one principal axis is perpendicular to the orbit plane (POP), a cyclic POP torque, possibly leading to large momentum storage requirements, may still exist. The only inertial vehicle with both low GG bias torques and low cyclic momentum accumulation is a vehicle where two moments of inertia are almost equal and the other axis is maintained perpendicular to the orbit plane.

Vehicles which are earth pointing(LV) present a different set of problems as regarding GG torques and momenta. A rotation of principal axes about the POP axis produces a POP bias torque. A rotation of the principal axes about the velocity vector produces a bias torque in vehicle space but a cyclic torque and momentum in inertial space. The accumulated momentum in vehicle space is also cyclic. However the gyroscopic torques which requires an exchange of momentum between the two vehicle axes in the orbit plane is an additional complicating factor to any proposed momentum management scheme. The fundamental potential advantage to momentum management for an LV vehicle is that, without implying momentum management should be the criterion for selecting LV, a gravity gradient torque free attitude can be found regardless of the inertia distribution. This study has concentrated on a vehicle which is oriented in the LV attitude and has the inertias and aerodynamic characteristics of the Dual Keel Space Station in the Initial Orbit Configuration(IOC) as shown in figure 1.

Momentum management is important to an LSS since it impacts momentum exchange actuator selection and sizing and Reaction Control System(RCS) requirements. The selected momentum management must adapt to parameter uncertainties in

inertias and aerodynamic torques. The resultant initial misalignment between the vehicle Z-axis and the local vertical must be removed by the momentum management scheme. If gravity gradient momentum management is selected, the gains are dependent on at least an approximate knowledge of vehicle inertias. This assumption is reasonable since, for an LSS, although the inertia tensor may not be known exactly, approximate values will always be available.

For an LSS, Control Moment Gyros(CMGs) compared to Reaction Wheels would appear to be the preferred momentum management actuators and will be baselined for this study. An RCS system will also be required for backup especially during buildup and docking but will not be considered in this study. Several momentum management schemes not involving mass expulsion could be considered. These include magnetic desaturation using torquer bars, aerodynamic desaturation using appendages, fluid momentum control, magnetic desaturation using magnetic coils wound around the structure and gravity gradient desaturation. Magnetic torquers are heavy and magnetic fields can contaminate payloads, aerodynamic panels produce very low torques and could interfere with payload viewing while the use of fluid momentum is still an unproven technique. Therefore gravity gradient desaturation is selected as the baseline. The only disadvantages are the maneuvers could interfere with earth pointing and vehicle angular acceleration could interfere with low-g experiments. However it is anticipated that these areas of potential conflict could be resolved much more easily than problems arising from any other momentum management techniques.

Possibly, the optimum momentum management scheme operates at orbital frequency which would filter the cyclic part of both aerodynamic and gravity gradient torques. Therefore sampling at orbital frequency allows the momentum management scheme to concentrate on removing the bias components of external torques and the accumulated momentum. This approach is discussed in reference 1 which examined the CDG planar space station as an example of a large space structure. The difficulty with this approach is, depending on the inertia differences and the amount of error, misalignment of the local vertical principal axis about the axis perpendicular to the orbit plane(POP) could

...PAGE IS
OF POOR QUALITY

DUAL KEEL — 1994

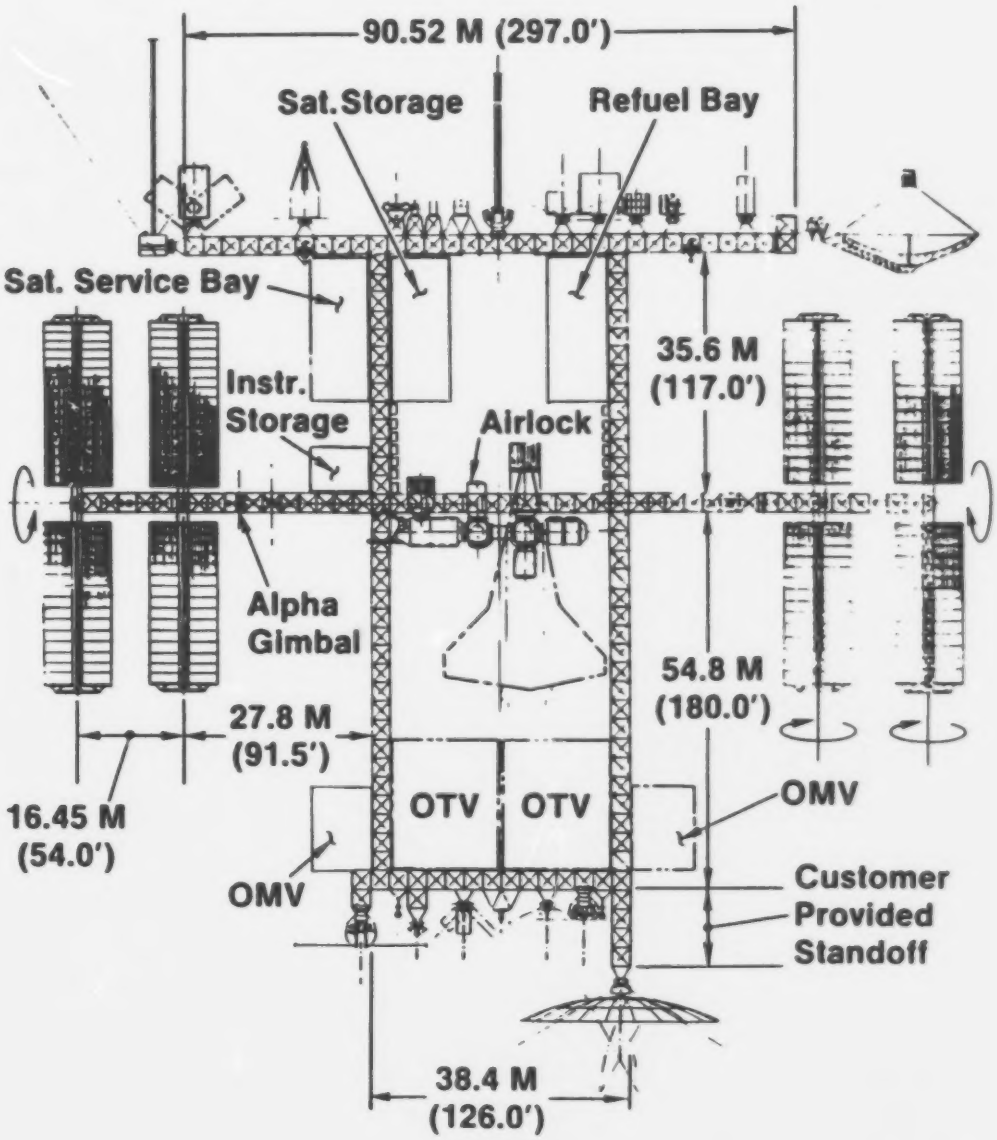

FIGURE 1 DUAL KEEL IN IOC CONFIGURATION

easily saturate the CMGs before the first orbit sample and resulting correction has been made. Therefore momentum sampling and gravity gradient maneuvers at higher than orbit frequency are required.

Classically in vehicles such as Skylab and Space Telescope, momentum management is performed at much lower frequencies than attitude control so that the two closed loop systems can be studied independently with momentum management being considered fixed for attitude control system studies and attiude control system response considered instantaneous and ideal for momentum management system studies. The large space structure such as the dual keel space station may have control bandwidths as low as .01 radians/sec so that although the momentum management scheme considered is based on ideal attitude system response, an upper limit to the number of corrections/orbit can be established. The tradeoff will be updating attitude and rate for momentum management sufficiently often to prevent saturation and keeping the update frequency low enough to maintain stability. After the transients have decayed, update at orbital or even sub-orbital frequencies may be adequate.

2.0 Development of concepts

A momentum management concept has been developed for the large space structure whose approximate attitude is the X-axis along the velocity vector, the Y-axis perpendicular to the orbit plane and the Z-axis pointing down at the earth. For the purposes of this study, three primary reference coordinate systems are defined. These are an orbit inertial reference system which is horizontal, down and POP at orbit noon, a local vertical(LV) set of coordinates which coincides with the reference at noon and a set of vehicle fixed coordinates which, for the cases studied to date is always approximately aligned to the LV. In addition, a set of coordinates fixed to the solar arrays is defined for the purpose of calculating solar array aerodynamic torques. Radiators and inertia changes due to solar array rotation with respect to the keel are not included in the simulation. Figure 2 shows the coordinate systems defined.

The initial goal of the momentum management concept developed was, to the extent feasible, eliminate the gravity gradient(GG) torque and the stored CMG momentum along the three vehicle axes. When the GG torques about vehicle X and Y-axes have been eliminated, vehicle principal axes have been aligned to the LV coordinate system. In the case investigated, no intelligence as to the angle between principal and control axes is required as maneuvers are computed autonomously. However the principal moments of inertia must be known approximately as inertia differences are part of the gains of the desaturation scheme developed. This scheme should be sufficiently robust so that errors of up to 10% between assumed and actual inertia differences can be tolerated. However the angles between principal and control axes were only about two degrees for the case considered. If these became very large, some intelligence might be required otherwise the CMGs could saturate before the momentum management scheme could align the principal axes with the LV coordinate system.

COORDINATE SYSTEMS

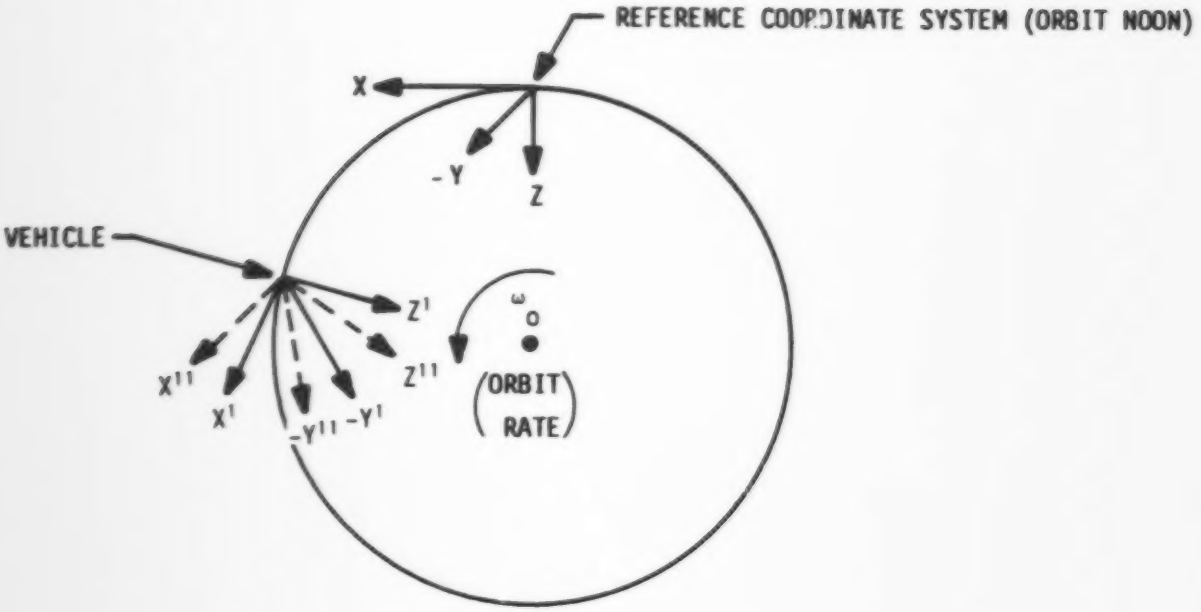

X, Y, Z - REFERENCE FRAME

X^{1}, Y^{1}, Z^{1} - LV FRAME

X^{11}, Y^{11}, Z^{11} - VEHICLE FRAME

FIGURE 2 REFERENCE COORDINATE SYSTEMS

3.0 Development of simulations without dynamics

In order to minimize complications arising from simulations, the first investigation was performed on a simulation shown in figure 3 which did not include vehicle dynamics. In this simulation, the gyroscopic torques are included only implicitly through system momentum. Several observations about the block diagram of figure 3 can be made. The total system momentum in inertial space is the initial system momentum plus the integral of external torques, initially defined in vehicle space, transformed to inertial space. Vehicle momentum is also defined in vehicle space and then transformed to inertial space. CMG momentum is first defined in inertial space as the difference of total momentum and vehicle momentum and transformed to vehicle space. The actual input to momentum management is the total vehicle momentum in inertial space. Orbital rate must be transformed to vehicle axes as these are generally not aligned with the LV frame and added to the rate command from momentum management to yield the total vehicle rate command. Since there is no vehicle dynamics, between momentum management updates, the vehicle rate is constant over each momentum management cycle with respect to the LV reference. The simulation was operated 120 times/orbit which makes the integration Δt about 47 seconds.

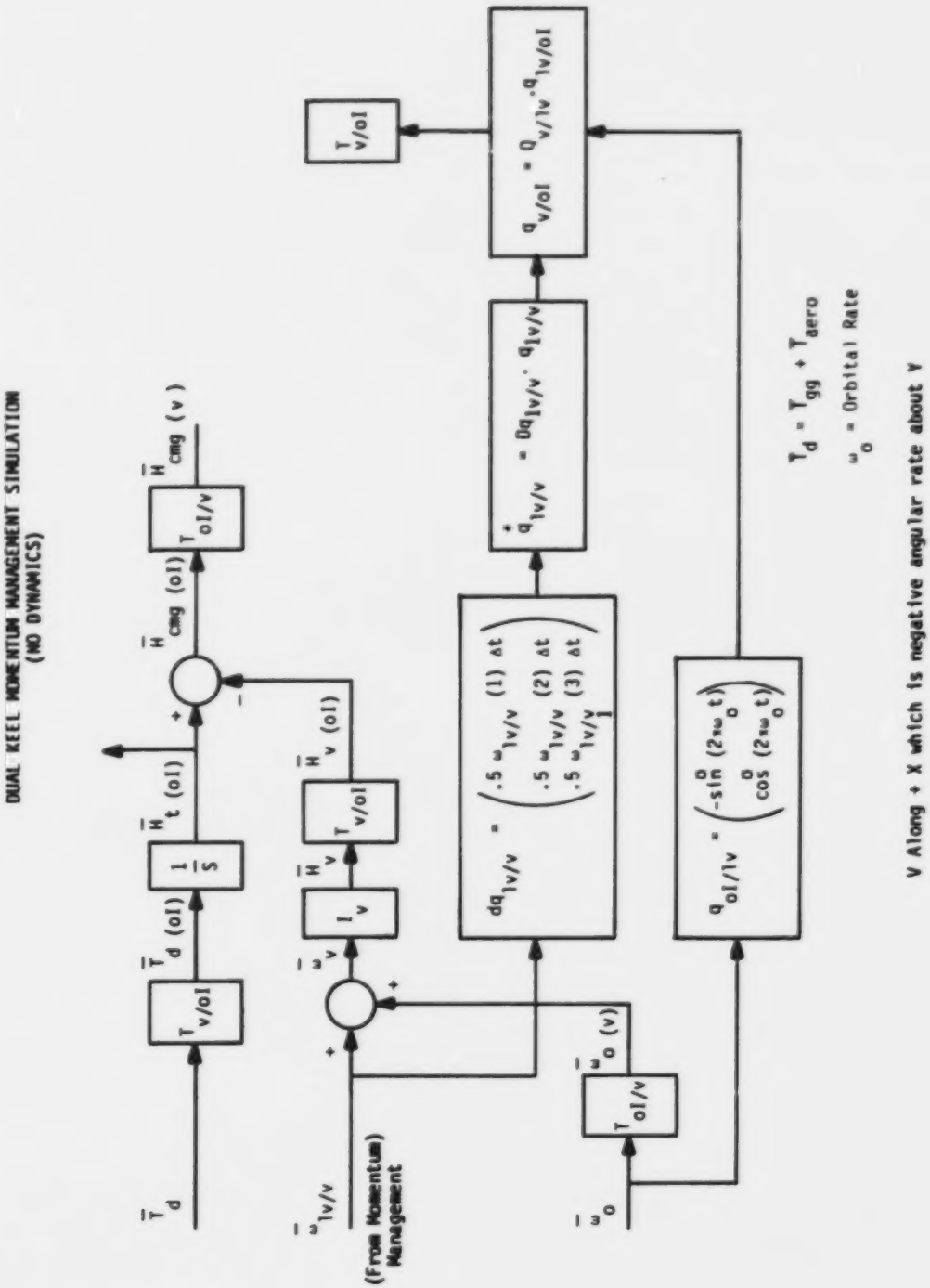

FIGURE 3 MOMENTUM MANAGEMENT SIMULATION WITHOUT DYNAMICS

4.0 Momentum Management Control Laws

The concept for momentum management is very similar for the POP and the in-orbit plane momentum(IOP). The schemes try to remove the gravity gradient torques and also any stored CMG momentum. The sampled parameters are the three components of CMG momenta in vehicle space and the three components of vehicle rate which are used to generate system momentum. The momentum bias is fixed in inertial space but transformed into vehicle space to produce the momentum error. The POP GG torque and momentum is corrected by maneuvers about the vehicle Y-axis while the IOP momentum is corrected by X-axis maneuvers. No maneuvers about the vehicle Z-axis are performed for momentum management as these would have only second order effectiveness. The system momentum is driven to a biased value which is zero(0) for the X-axis momentum and $-\omega_0 I_{yp}$ for the Y-axis momentum where I_{yp} is the best estimate of vehicle Y-axis principal inertia.

If the Z principal axis is rotated away from the local vertical by a rotation about the Y-axis by an angle assumed constant over the momentum management sample interval(T_m), the change in momentum over that interval is given by equation (1).

$$\bar{H}_{ny} - \bar{H}_{(n-1)y} = 3\omega_0^2 \Delta I_y \theta_{yp} T_m \qquad (1)$$

The angle to be commanded, where no momentum management maneuver was active during the previous interval, is given by equation (2). G_θ contains both a gain factor k_θ and the estimate of the inertia difference between vehicle X and Z principal moments of inertia and is defined by equation (3)

$$\theta_{yc} = \frac{G_\theta (H_{ny} - H_{(n-1)y})}{T_m} \qquad (2)$$

$$G_\theta = \frac{K_\theta}{3\omega_o^2 \, \Delta I_{y(est)} \, T_m} \tag{3}$$

Equation (3) requires one additional modification in the case where the vehicle was making a momentum management maneuver during the previous momentum management computation cycle. Assuming that the vehicle rate was equal to the commanded constant rate, the change in momentum is given by equation (4). The angle of the principal axis from the LV at the beginning of the momentum management cycle is given by equation (5) while the estimate of the current angle, which is the error angle to be removed, is given by equation (6)

$$H_{ny} - H_{(n-1)y} = 3\omega_o^2 \, \Delta I_y \left(\theta_{yp} \, T_m + \frac{\dot{\theta}_{yp} \, T_m^2}{2}\right) \tag{4}$$

$$\theta_{yp} = G_\theta \left(H_{ny} - H_{(n-1)y}\right) - \frac{\dot{\theta}_{yp} \, T_m}{2} \tag{5}$$

$$\theta_{yc} = \theta_{yp} + \dot{\theta}_{yp} \, T_m = G_\theta \left(H_{ny} - H_{(n-1)y}\right) + \frac{\dot{\theta}_{yp} \, T_m}{2} \tag{6}$$

In addition to the commanded angle to remove the GG torque, a constant rate to remove the current momentum error during the next momentum management computation cycle must also be commanded. The change in momentum due to a constant rate over the next momentum management time interval is given by equation (7).

$$H_{(n+1)y} - H_{ny} = 3\omega_o^2 \, \Delta I_y \, \frac{T_m^2}{2} \, \dot{\theta}_{yh} \tag{7}$$

Therefore the rate to remove a momentum error again includes a gain term, K_h, and the estimate of the inertia difference between X and Z vehicle principal axes and is given by equation (8).

$$\dot{\theta}_{yh} = \frac{K_h \; H_{ny}}{3\omega_o^2 \, \Delta I_{y(est)} \, .5T_m^2} = G_h \, H_{ny} \tag{8}$$

The total rate to be commanded is given by equation (9) and represents the Y-axis momentum management rate command for the next momentum management time interval.

$$\dot{\theta}_{yc} = \frac{-\theta_{yp}}{T_m} - \dot{\theta}_{yh} \tag{9}$$

The estimate on the gains was that K_θ should be about one(1.) since it is desired to eliminate gravity gradient torque producing offset as quickly as possible. The momentum gain K_h should be fairly low since it is destabilizing. The values investigated were in the range of 0.2 to 0.5. The actual values

selected were one(1.) for K_θ and 0.2 for K_h.

IOP momentum is handled in a similar manner to the POP momentum despite the fact that significant differences exist between the physics of the POP axis torques and the IOP axes torques. The first major difference is the existence of gyroscopic torques which causes a momentum exchange between the vehicle X and Z axes. Therefore despite the fact that, if the vehicle principal axes are approximately aligned with the LV, no gravity gradient torques exist on the vehicle Z-axis, momentum is accumulated via the gyroscopic torque. The second major difference is that due to gyroscopic torque, an offset of the vehicle Z-principal axis from the orbit plane by a X-rotation, while producing a GG bias torque along the vehicle X-axis, produces cyclic CMG momentum. Therefore it is less critical, for this configuration, to eliminate vehicle X-axis GG torque than to remove Y-axis GG torque which produces ever increasing CMG momentum leading to potential saturation. For an LV vehicle without external disturbances, system momentum remains constant in inertial space. Hence CMG momentum stored along the vehicle Z-axis must be stored along the vehicle X-axis after 90° orbital motion. This momentum interchange makes it possible to eventually desaturate both X and Z-axes CMG momentum with an X-axis rotation.

The control law for the IOP momentum is essentially identical to that for the POP case except that the sensed angle to remove GG torque must include a compensation for the gyroscopic torque. Equation (6) is therefore modified to become equation (10) where the total Z-axis momentum is assumed to be the Z-axis CMG momentum and G_θ uses I_{xp}.

$$\theta_{xc} = G_\theta(H_{nx}-H_{(n-1)x} - \omega_o H_{zavg} T_m) + \frac{\dot{\theta}_{xp} T_m}{2} \qquad (10)$$

The gyroscopic torque causes two additional differences between the POP and the IOP desaturation schemes. Since Z-axis momentum becomes X-axis momentum within 90 orbital degrees, a series of X-axis maneuvers can eliminate both X and Z momentum. The fact that the gyroscopic torque goes from zero(0) to its

peak within 90 orbital degrees limits the momentum management sample interval for the IOP case to a time which is much smaller than one-quarter orbit. The POP momentum management sample interval can be extended to one or more entire orbits. If desaturation at orbital frequency of the IOP momentum would be required, the method of reference 1 which precomputes the maneuver profile for the entire orbit would be adequate. However, the cases investigated to date indicate that once the vehicle attitude has been trimmed, adjustment of the IOP momentum is not required for many orbits. The lower limit on the momentum management sample interval is the desire to separate momentum management and attitude control bandwidths to insure stability. The Z-axis momentum used in equation (10) is the average sampled value over the last momentum management sample interval. Figure 4 represents the block diagram equivalent of the proposed momentum management scheme.

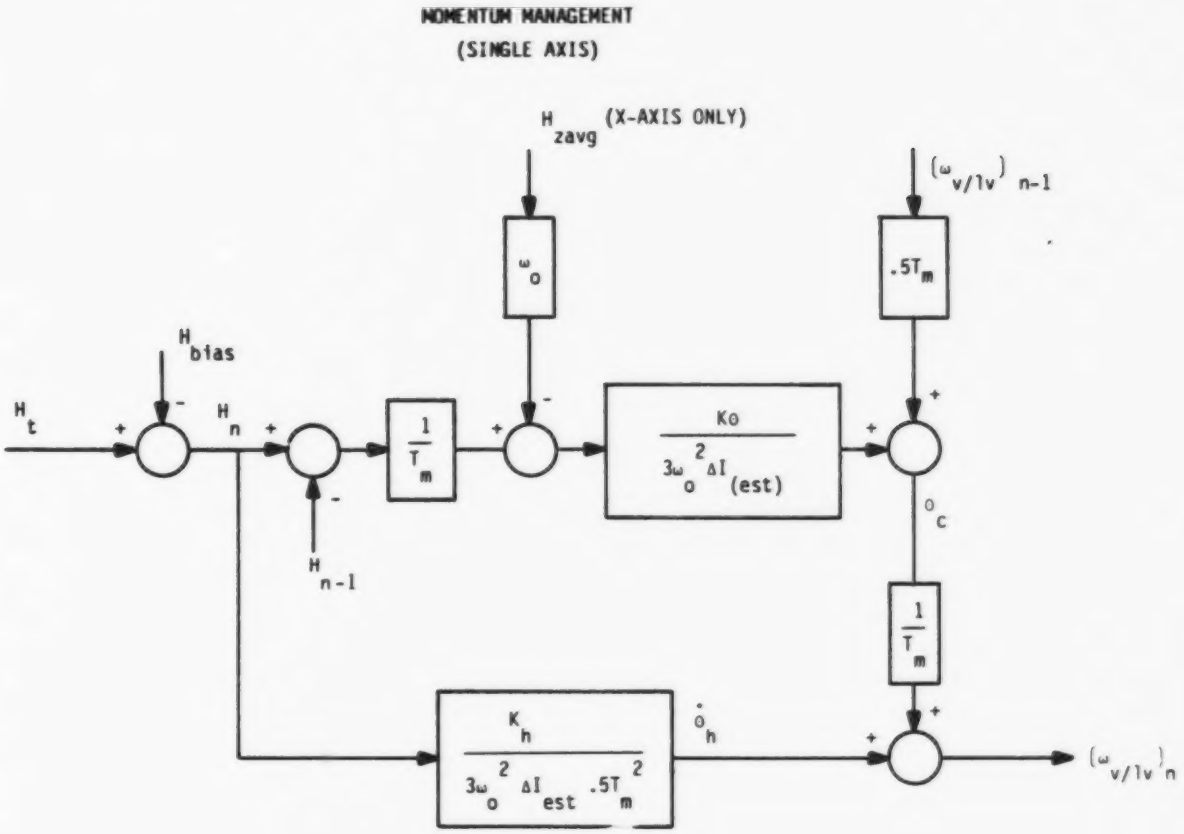

FIGURE 4 MOMENTUM MANAGEMENT BLOCK DIAGRAM

5.0 Simulation results without dynamics

Figure 5 shows the POP momentum with the momentum management operating at 20 samples/orbit for the first 2 orbits and once/orbit after orbit 3. During orbit 3 which is the transition orbit, no maneuvers are performed accounting for the increase in momentum. Figure 6 shows the same momentum profile concentrating on the first two(2) orbits where the transients occur. Figure 7 shows the POP axis CMG momentum with an incorrect initial inertia estimate leading to a CMG bias. Figure 8 shows the POP CMG momentum with the initial incorrect inertia estimate but with an adaptive update scheme every fifth orbit to eliminate CMG momentum bias by changing the inertia estimate. Figure 9 shows the IOP momentum with momentum management only during the first two orbits. There are no X-axis maneuvers performed during orbits 3 - 20 and momentum is increasing only very slowly so that,theoretically, no further maneuvers about the X-axis would be required for at least 100 orbits. Even if inertias, atmospheric density and beta angles would slowly vary, the proposed momentum management scheme would still be very effective. This is primarily due to the fact of the selected vehicle configuration with fairly large inertia differences but very low IOP aerodynamic torques and resultant momentum, as shown in figure 10, since the center of pressure of the balanced solar array configuration is close to the center of mass. Therefore desaturation maneuvers using GG torques are primarily to counteract torque and momentum due to GG torques which is optimum for the performance of a GG desaturation scheme. Figure 11 shows the performance of the IOP momentum management scheme after vehicle X and Z axes CMG momentum has been allowed to accumulate over many orbits. The proposed method easily removes the accumulated IOP momentum during two active orbits. Figure 12 shows the same IOP response concentrating on the first two orbits.

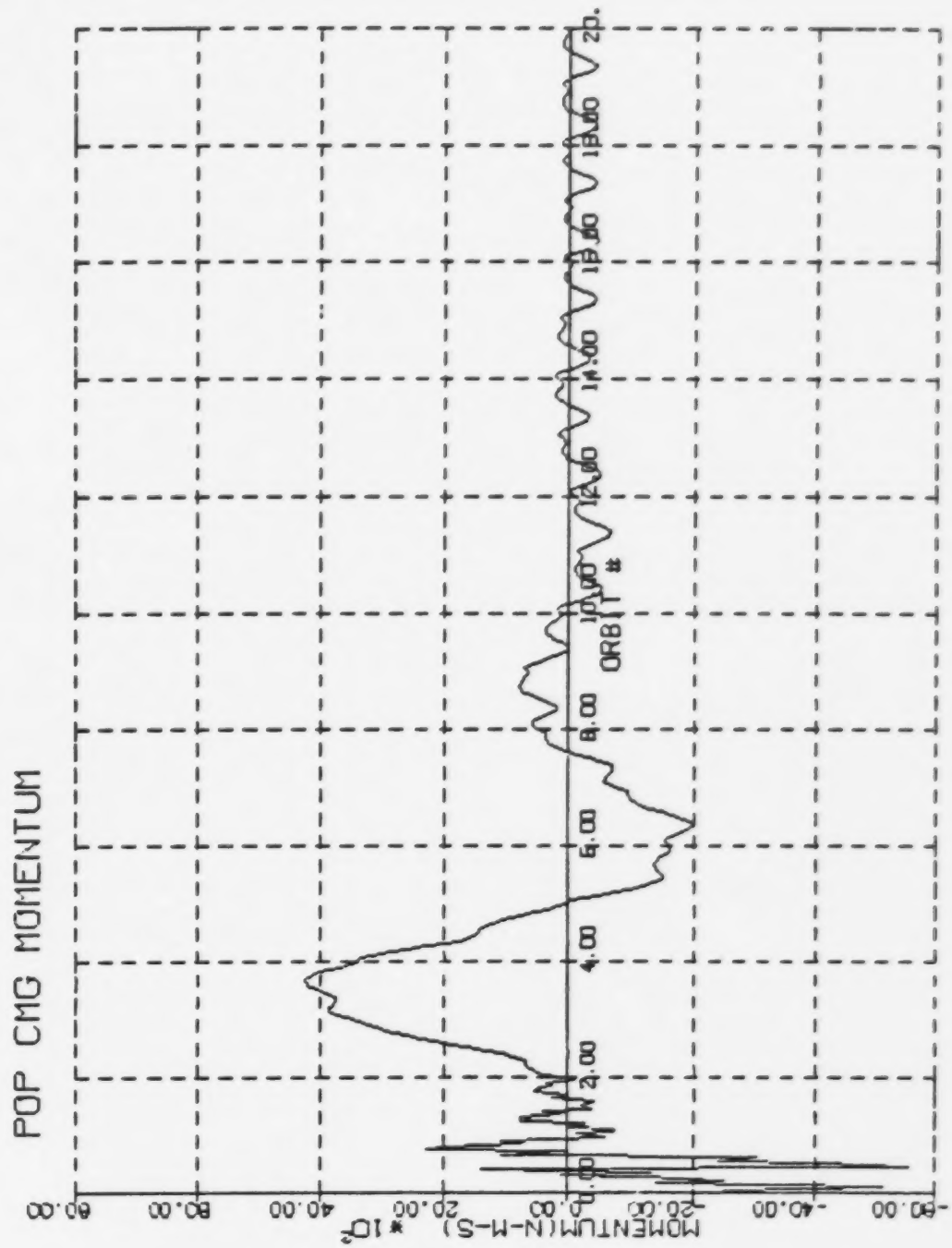

FIGURE 5 POP AXIS MOMENTUM MANAGEMENT RESPONSE

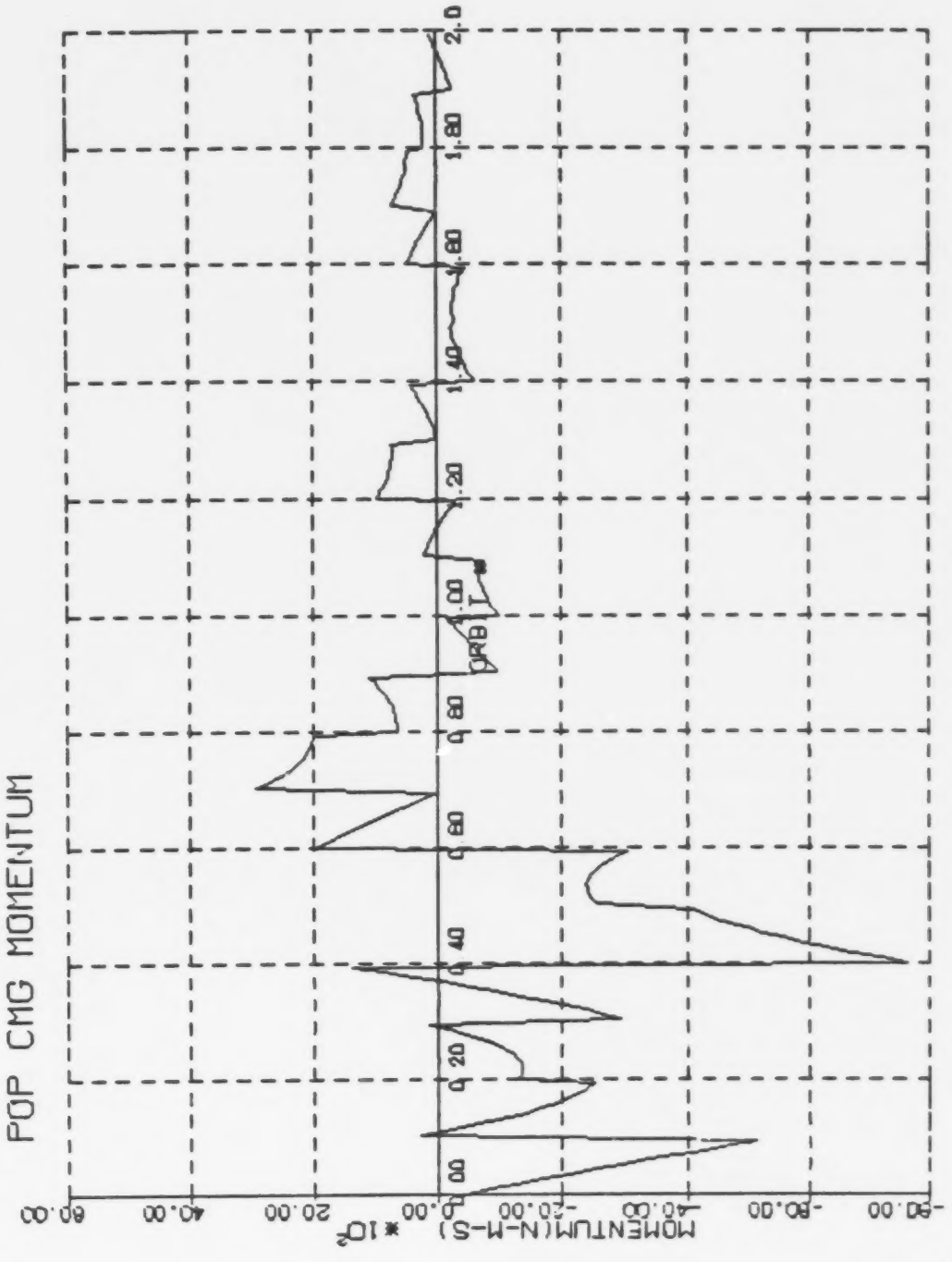

FIGURE 6 POP AXIS RESPONSE FOR FIRST 2 ORBITS

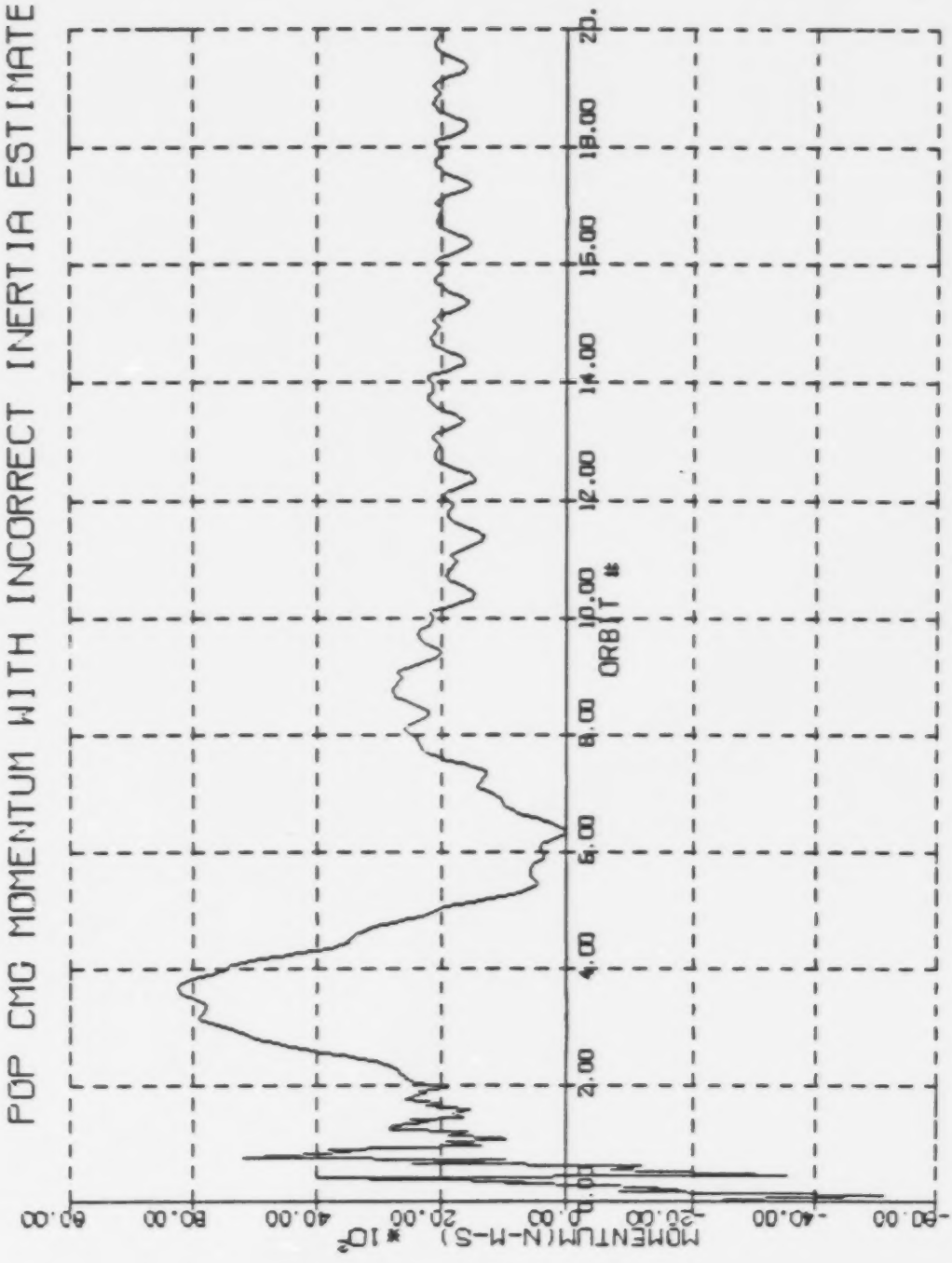

FIGURE 7 POP RESPONSE WITH INCORRECT INERTIA ESTIMATE

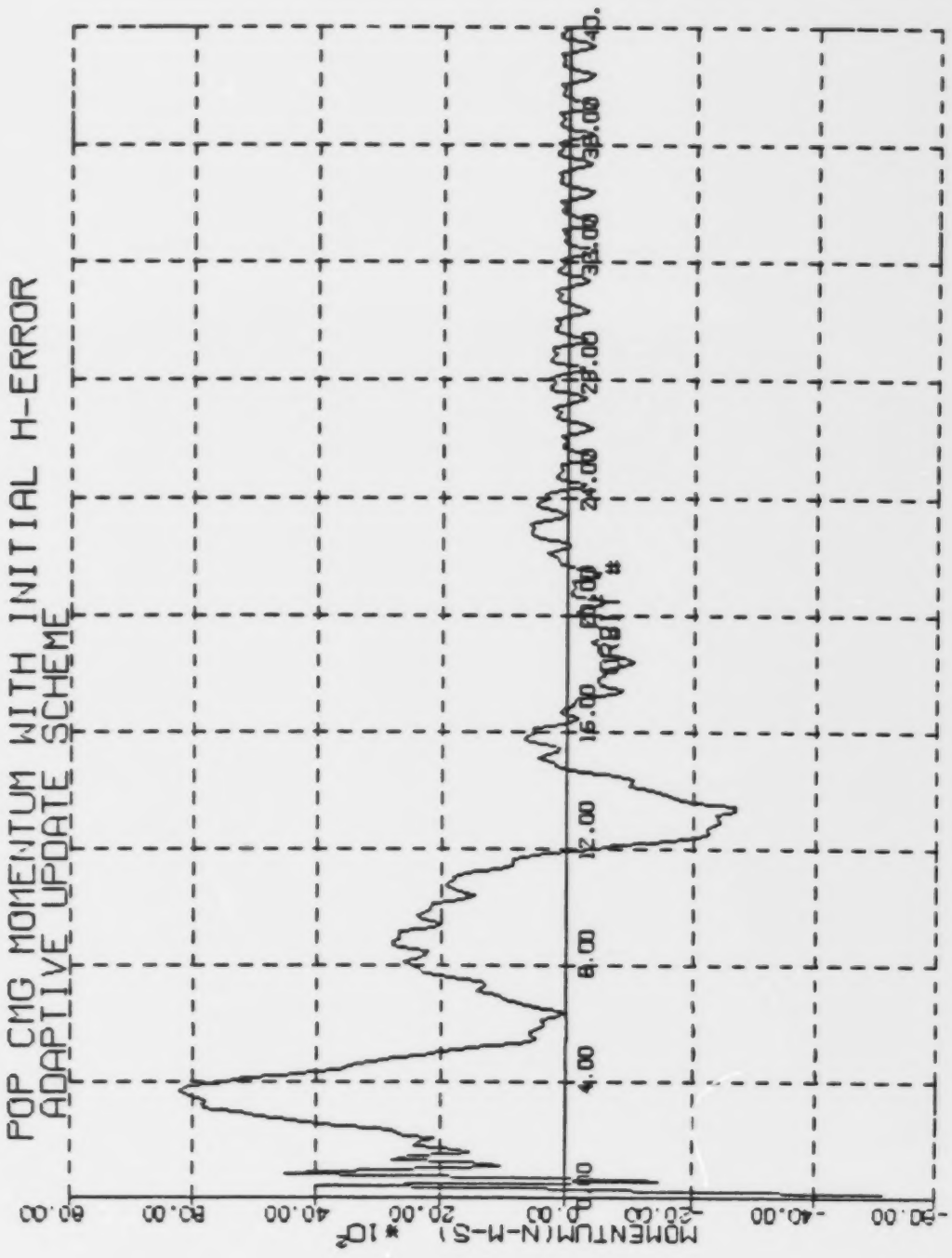

FIGURE 8 POP RESPONSE WITH INCORRECT INERTIA ESTIMATE AND ADAPTIVE UPDATE SCHEME

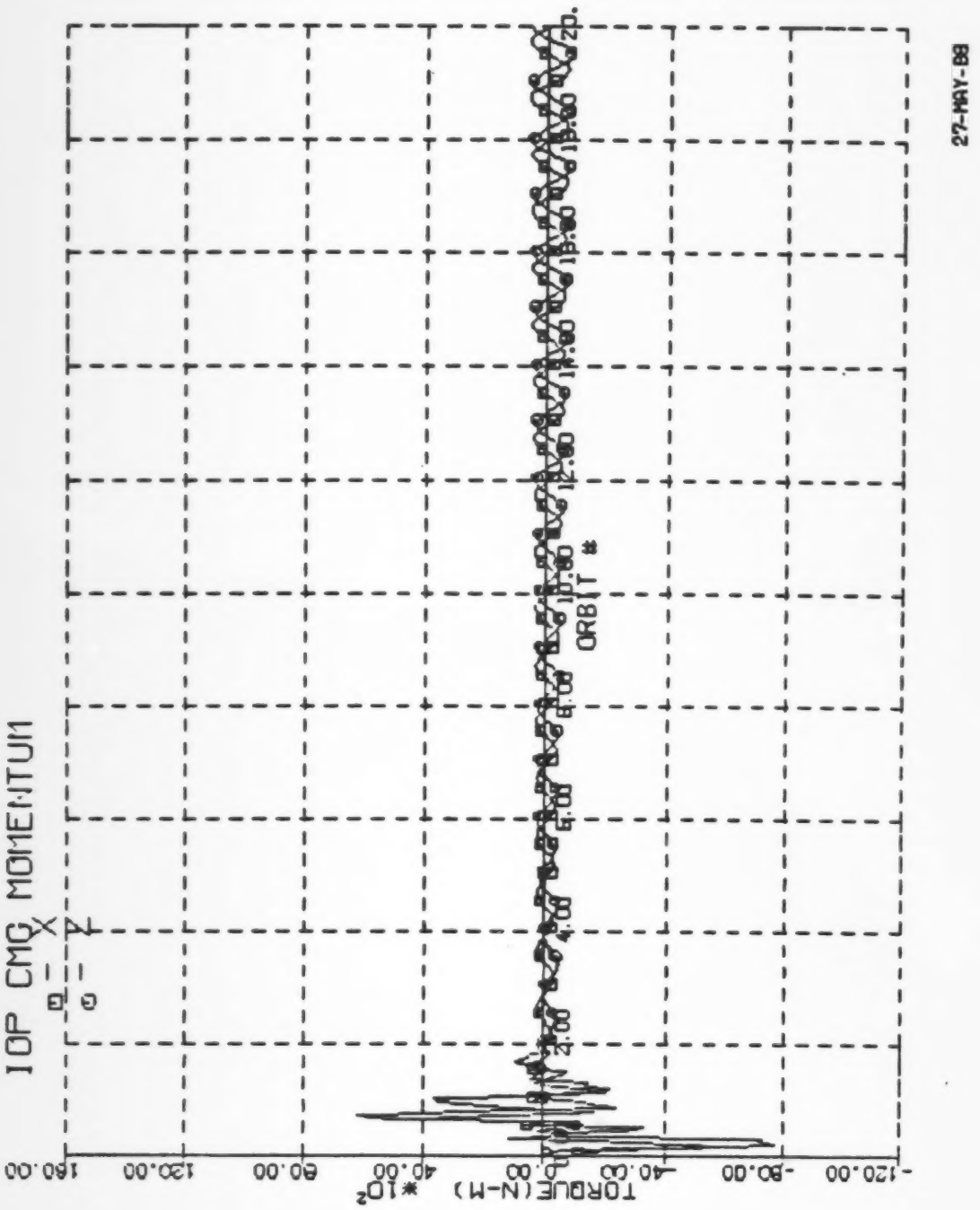

FIGURE 9 IOP AXES MOMENTUM MANAGEMENT RESPONSE

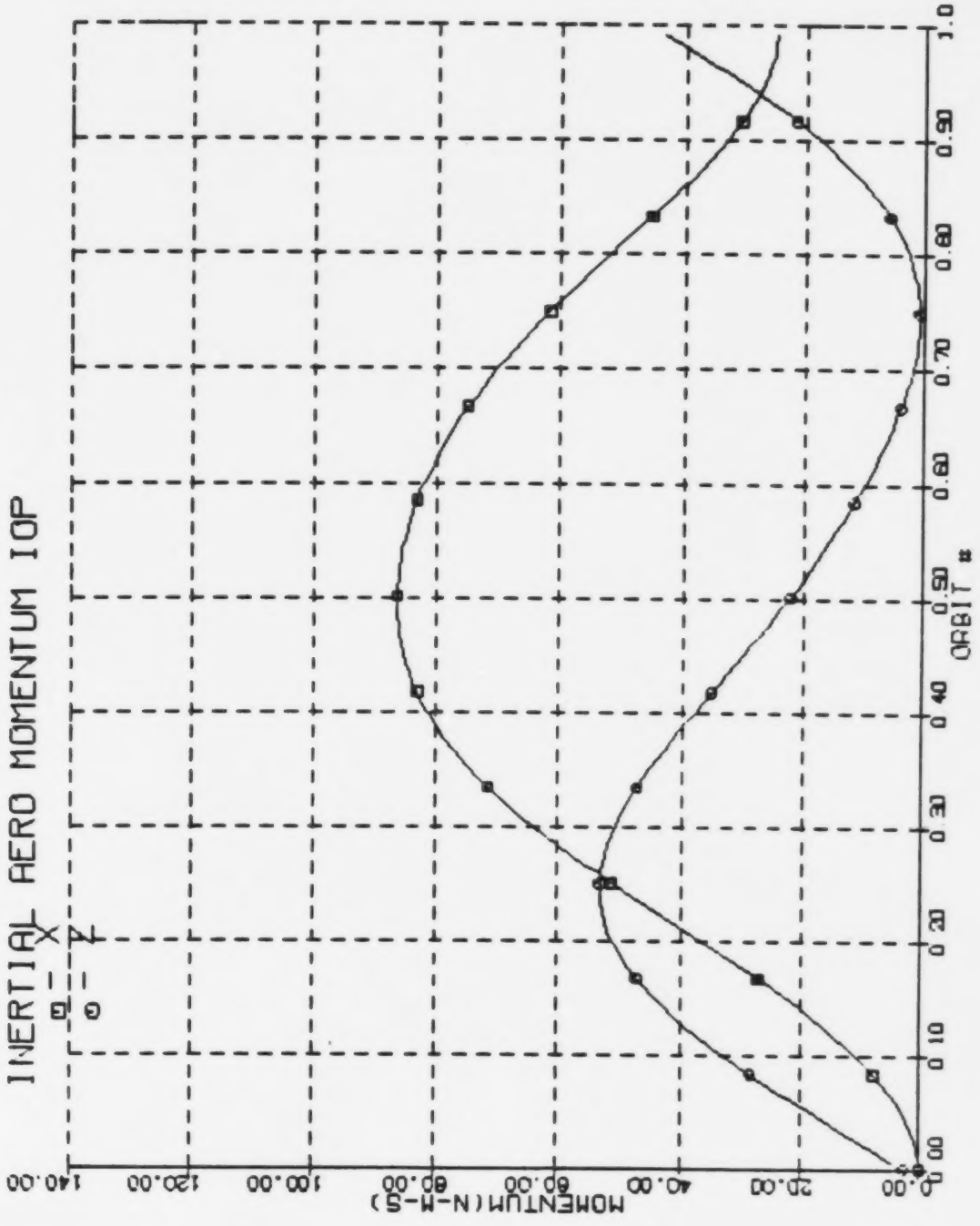

FIGURE 10 IOP AXES AERODYNAMIC TORQUE INDUCED MOMENTUM

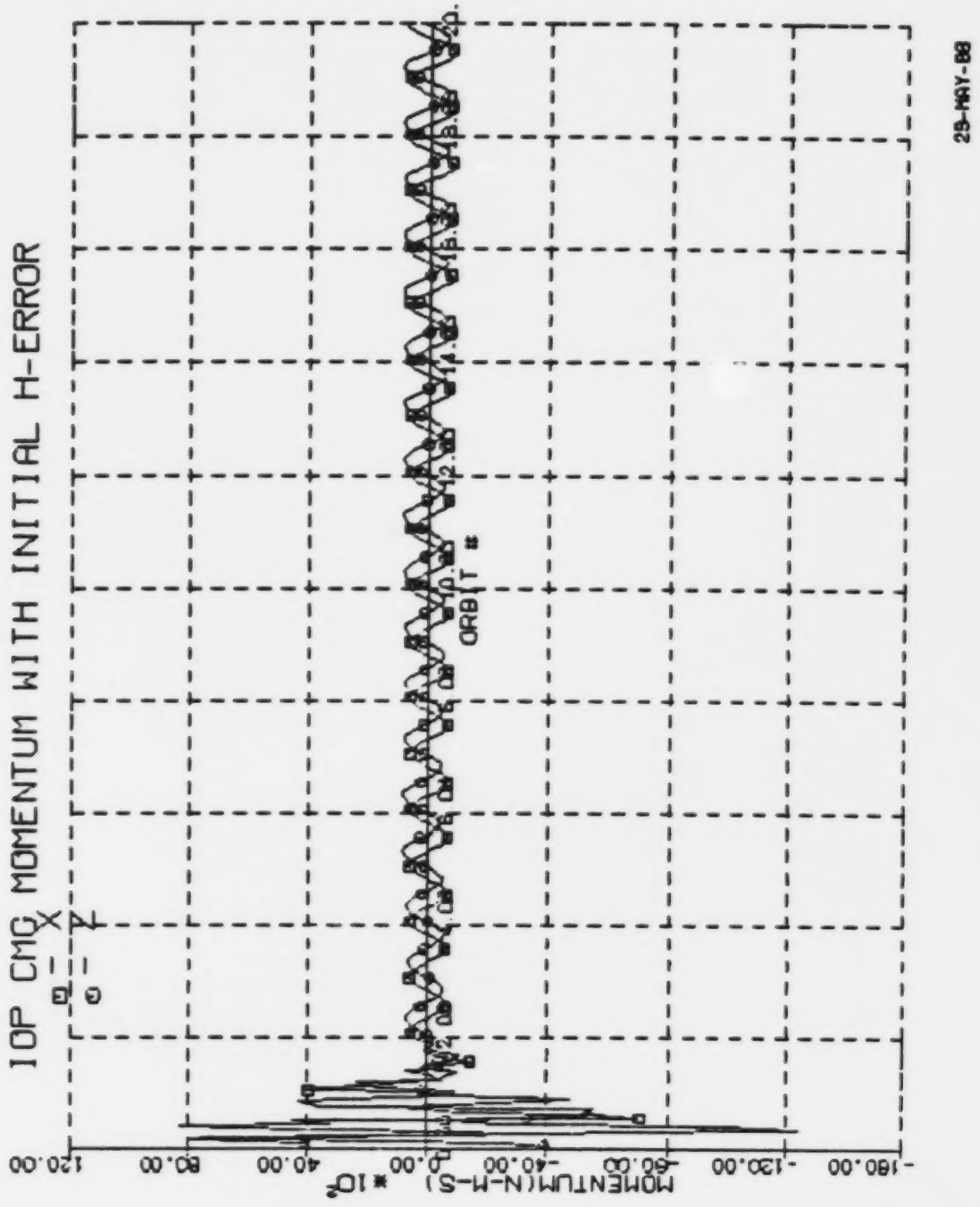

FIGURE 11 IOP MOMENTUM MANAGEMENT WITH INITIAL ACCUMULATED IOP MOMENTUM

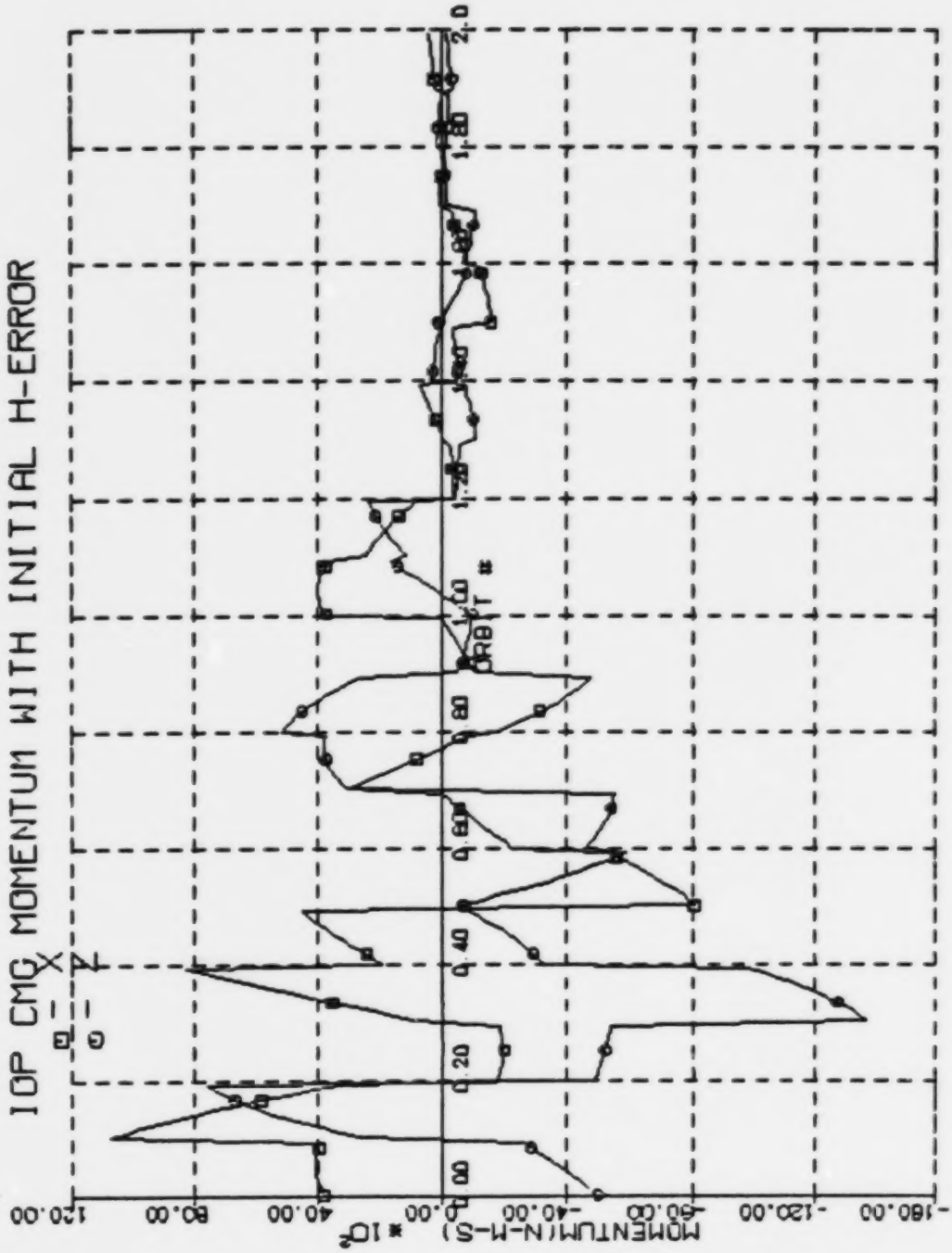

FIGURE 12 IOP AXES RESPONSE FOR FIRST 2 ORBITS

6.0 Verification of results with vehicle dynamics

The momentum management techniques developed were now verified using the more detailed model of figure 13 which includes vehicle dynamics. The differences include errors between the commanded and actual vehicle rates, explicit gyroscopic torques acting as a disturbance, a second order rate and position vehicle control law on all vehicle axes, an actual vehicle rate command emanating from momentum management and CMG momentum in vehicle space as the integral of control torques. The vehicle control law used a damping ratio of .9 and a natural frequency ranging from .01 radians/sec to .01 hz. The simulation was run at 600 steps/orbit compared to 120 steps/orbit without dynamics which represents a Δt of about nine(9) seconds. With the .01 hz control bandwidth, the momentum response was identical to that without dynamics. When the vehicle control bandwidth was lowered to .01 radians/sec, an insignificant change in the response could be seen. Therefore the momentum management concept was verified in the presence of dynamics. The simulation of figure 13 assumes CMG torque is identical to that demanded.

The next order of verification was to include the Kennel steering law as described in reference 2. The CMG configuration utilized was six(6) Double Gimbal Control Moment Gyros(DGCMGs) parallel mounted with each CMG having 3500ft-lb-sec(4650n-m-sec) angular momentum. The dynamics of the individual CMG rate loops which are about 3Hz were not included. The response of the CMGs were considered instantaneous since including detailed CMG models would greatly complicate and slow down the simulation without providing additional information.

No change in the momentum time history was observed using the simulation of Figure 14 with the Kennel Steering law compared to the response using the simulation of figure 13 where actual torque equals commanded torque. This result is expected since the typical gimbal rates commanded during an orbit where momentum management is active, such as orbit one(1), are well below the assumed maximum capability of 3.5deg/sec. Typical maximum inner and outer gimbal rates are shown in figures 15 and 16. An observation on figure 14, is that the simulation reverses sign in the vehicle control law causing the

definition of CMG momentum to be the negative of the Kennel steering law as defined in reference 2.

DUAL KEEL MOMENTUM MANAGEMENT
SIMULATION WITH VEHICLE DYNAMICS

$\bar{T}_d = \bar{T}_{gg} + \bar{T}_{gy} + \bar{T}_{aero}$ $\quad \bar{\omega}_c = \bar{\omega}_{v/lv} + \bar{\omega}_o$

(FROM MOMENTUM MANAGEMENT)

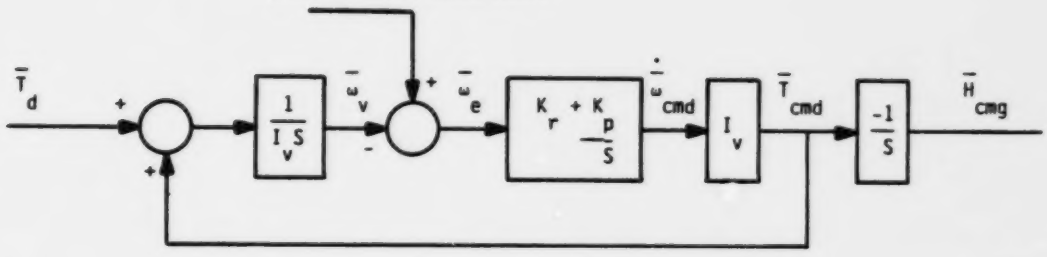

$\bar{H}_{tv} = I_v \bar{\omega}_v + \bar{H}_{cmg}$

$\bar{T}_{gy} = -\bar{\omega}_v \times \bar{H}_{tv}$

$$dq_{oI/V} = \begin{pmatrix} .5\omega_v\ (1)\ \Delta t \\ .5\omega_v\ (2)\ \Delta t \\ .5\omega_v\ (3)\ \Delta t \\ 1 \end{pmatrix}$$

$q^{+}_{oI/v} = Dq_{oI/v} \cdot q_{oI/v}$

$\bar{H}_{t(oI)} = T_{v/oI} \cdot \bar{H}_t$ (USED FOR MOMENTUM CONTROL)

FIGURE 13 SIMULATION WITH VEHICLE DYNAMICS

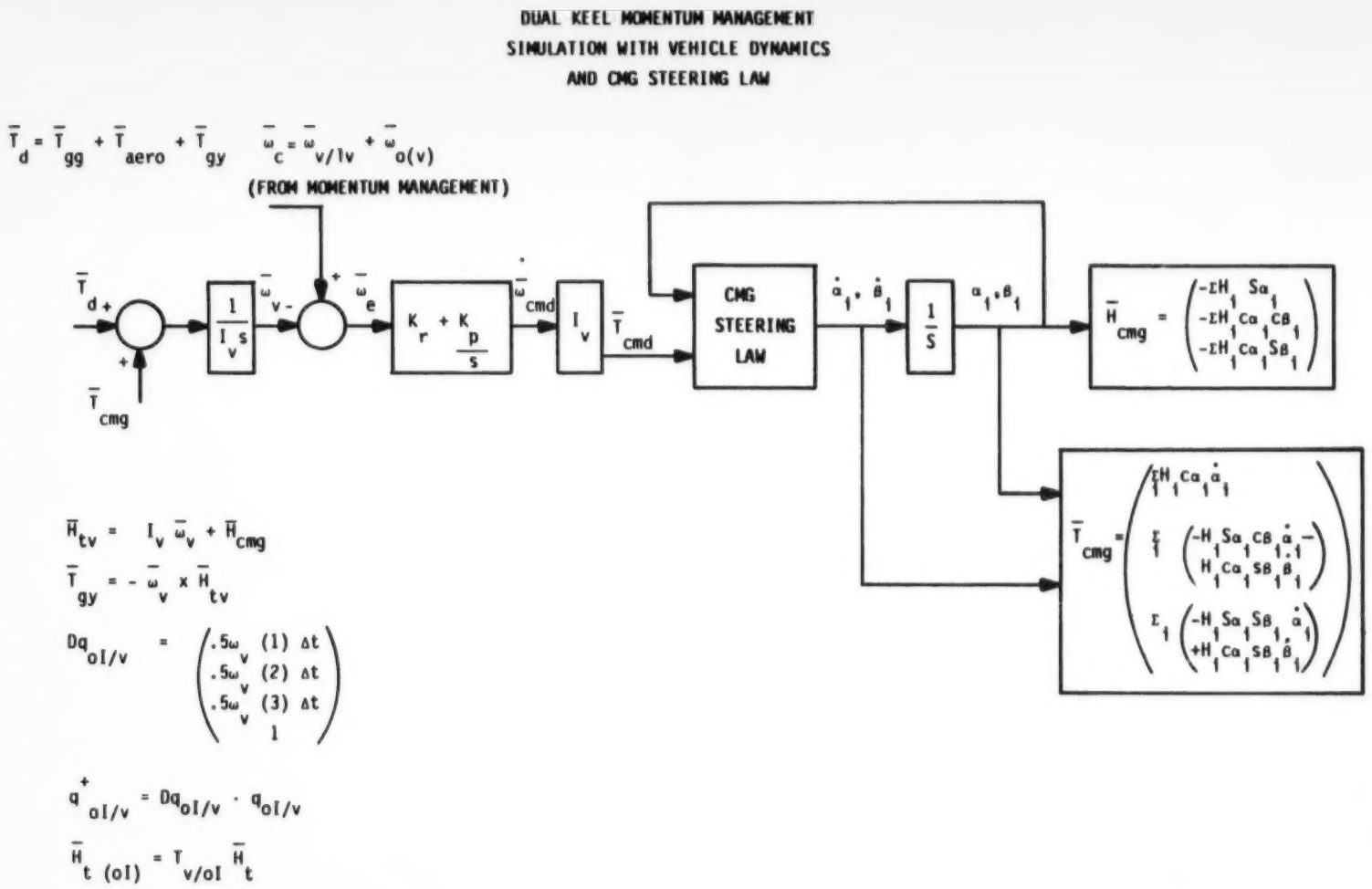
DUAL KEEL MOMENTUM MANAGEMENT
SIMULATION WITH VEHICLE DYNAMICS
AND CMG STEERING LAW
$\bar{T}_d = \bar{T}_{gg} + \bar{T}_{aero} + \bar{T}_{gy}$
$\bar{\omega}_c = \bar{\omega}_{v/Iv} + \bar{\omega}_{o(v)}$
(FROM MOMENTUM MANAGEMENT)
$\bar{T}_d$
$\bar{T}_{cmg}$
$\frac{1}{I_v s}$
$\bar{\omega}_v$
$\bar{\omega}_e$
$K_r + K_p/s$
$\dot{\bar{\omega}}_{cmd}$
I_v
$\bar{T}_{cmd}$
CMG STEERING LAW
$\dot{\alpha}_1, \dot{\beta}_1$
$\frac{1}{S}$
α_1, β_1
$\bar{H}_{cmg} = \begin{pmatrix} -\Sigma H_1 S\alpha_1 \\ -\Sigma H_1 C\alpha_1 C\beta_1 \\ -\Sigma H_1 C\alpha_1 S\beta_1 \end{pmatrix}$
$\bar{T}_{cmg} = \begin{pmatrix} \Sigma H_1 C\alpha_1 \dot{\alpha}_1 \\ \Sigma_1 \begin{pmatrix} -H_1 S\alpha_1 C\beta_1 \dot{\alpha}_1 - \\ H_1 C\alpha_1 S\beta_1 \dot{\beta}_1 \end{pmatrix} \\ \Sigma_1 \begin{pmatrix} -H_1 S\alpha_1 S\beta_1 \dot{\alpha}_1 \\ +H_1 C\alpha_1 S\beta_1 \dot{\beta}_1 \end{pmatrix} \end{pmatrix}$
$\bar{H}_{tv} = I_v \bar{\omega}_v + \bar{H}_{cmg}$
$\bar{T}_{gy} = -\bar{\omega}_v \times \bar{H}_{tv}$
$Dq_{oI/v} = \begin{pmatrix} .5\omega_v (1) \Delta t \\ .5\omega_v (2) \Delta t \\ .5\omega_v (3) \Delta t \\ 1 \end{pmatrix}$
$q^+_{oI/v} = Dq_{oI/v} \cdot q_{oI/v}$
$\bar{H}_{t\,(oI)} = T_{v/oI}\, \bar{H}_t$

FIGURE 14 SIMULATION WITH VEHICLE DYNAMICS, 6 DGCMGs AND KENNEL STEERING LAW

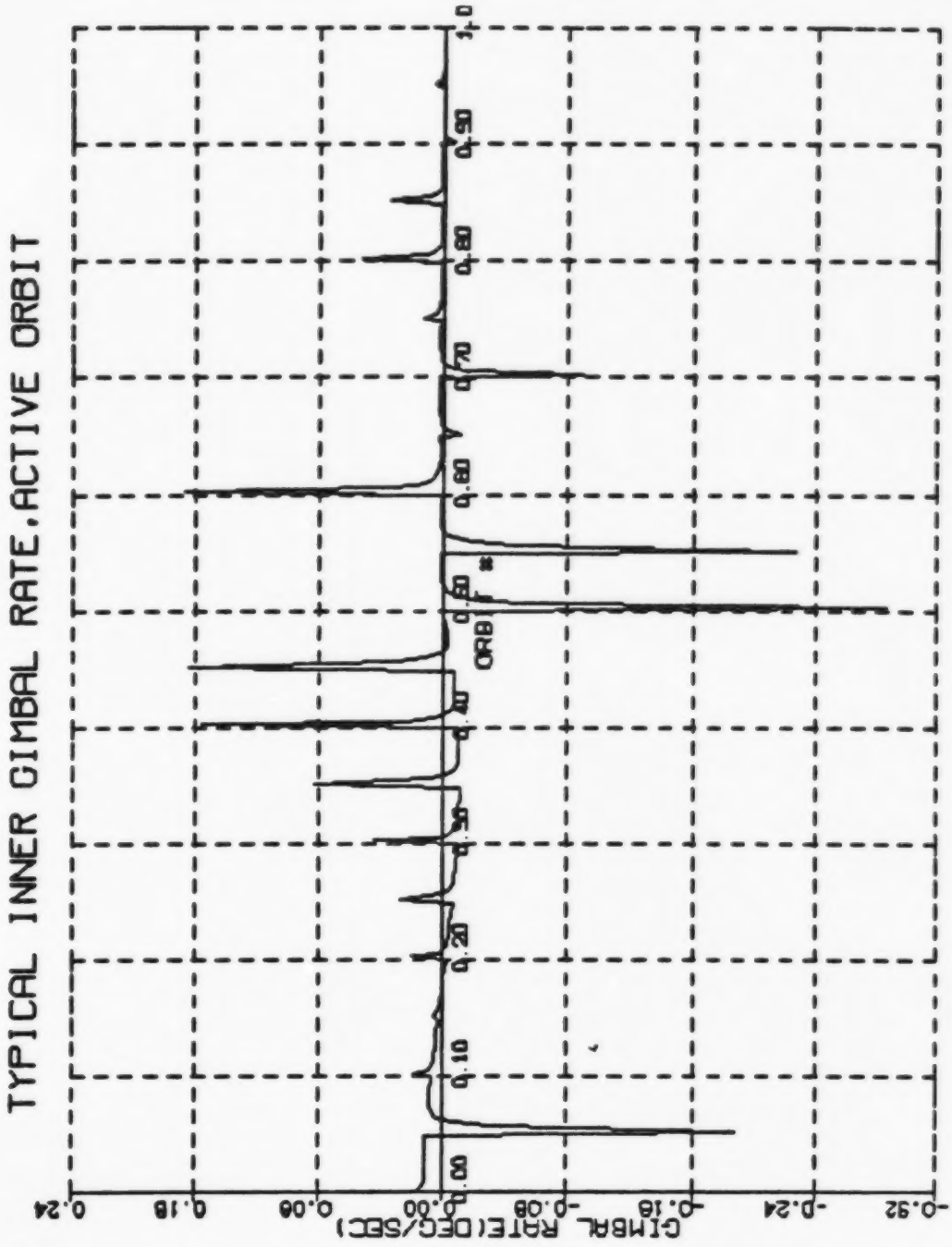

FIGURE 15 TYPICAL INNER GIMBAL RATE PROFILE DURING ACTIVE ORBIT

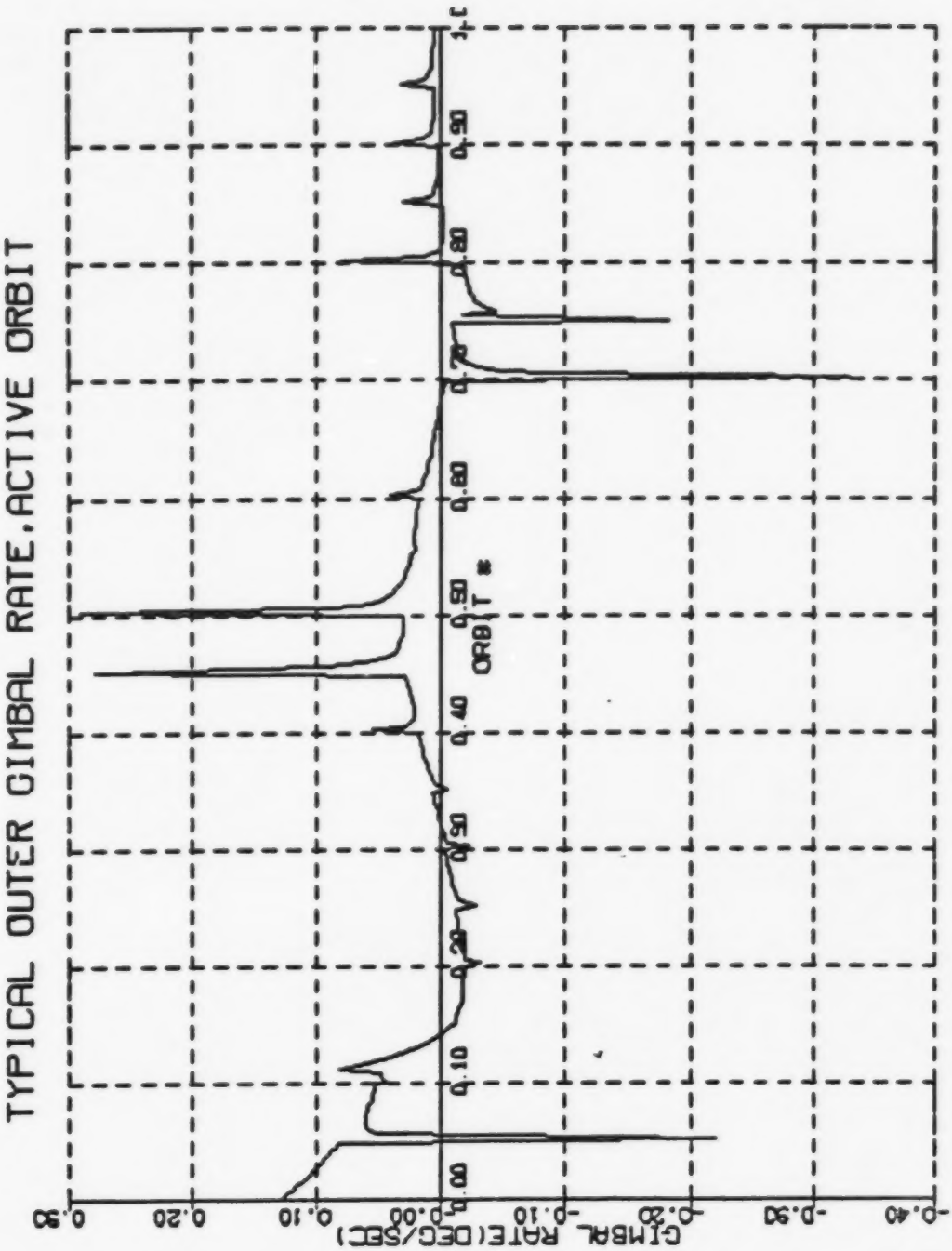

FIGURE 16 TYPICAL OUTER GIMBAL RATE PROFILE DURING ACTIVE ORBIT

7.0 Conclusions

Momentum Management using GG desaturation is feasible for a Large Space Structure maintained in a nominal LV attitude. The representative LSS used for the purposes of this study was the Dual Keel Space Station as shown in figure 1. The mission profile is such that the minimum principal axis was POP, the intermediate axis was LV and the maximum moment of inertia was along the velocity vector. The ratios of principal moments of inertia were approximately 1.5 between miminum, intermediate and maximum respectively which is far removed from the ideal long slender vehicle along LV. On the other hand, the fact that the solar arrays and radiators are almost balanced about the center of mass means that aerodynamic torques are quite small. Therefore gravity gradient desaturation works predominately against gravity gradient torques.

The desaturation scheme operates by eliminating the sensed GG bias torque and driving the system momentum to the desired value about two vehicle axes. The desired total momentum is $-\omega_0 I_{yp}$ about the vehicle Y-axis and zero(0) about the vehicle X-axis. No desaturation maneuvers about the vehicle Z-axis are performed. In order to prevent CMG saturation about the vehicle Y-axis due to the initial deviation of the Z-principal axis from LV, the initial corrections are performed at 20 corrections/orbit. This update frequency will be reduced to once/orbit once the initial attitude excursions have damped out and the principal axes are very close to their ideal orientation which is along the velocity vector, POP and LV respectively.

Almost the identical algorithm is used for correcting torque and momentum about the vehicle X-axis despite the fact that for this configuration the danger of saturation does not exist. The differences are that the sensed X-axis bias torque must be corrected for gyroscopic torque and that when the POP desaturation reverts to once/orbit update, IOP desaturation ceases and will only be required as momentum builds up IOP. Should IOP desaturation at orbit frequency be required, the method proposed in reference 1 would be satisfactory. In removing the accumulated vehicle X-axis momentum at 20 updates/orbit, due to the exchange of momenta in vehicle space between the two axes IOP, the vehicle Z-axis momentum would also be removed.

Since the system momentum along the vehicle Y-axis depends on the estimate of the Y-axis principal inertia, errors in this estimate lead to non-zero steady state Y-axis CMG momentum. This can be sensed and adaptively update the estimate of I_{yp} which through the momentum management scheme drives the Y-axis CMG momentum to zero(0). The X-axis principal inertia only comes in as a gain and errors in that estimate could only be determined with great difficulty. In general, the scheme should be robust to at least 10% principal inertia estimates.

8.0 Summary

A simple GG momentum management scheme has been has been developed for a large space structure similar to the Dual Keel Space Station in the IOC configuration. The algorithm is based on estimates of the principal moments of inertia and, by commanding rates about the vehicle X and Y-axes, drives both the GG torques and accumulated CMG momenta about vehicle X and Y-axes to zero(0). Due to gyroscopic torques, the selected algorithm in driving vehicle X-axis momentum to zero will also drive accumulated vehicle Z-axis momentum to zero(0). This algorithm has also been shown to be robust in the presence a vehicle control bandwidth as low as .01 radians/sec and uncertainties in knowledge of principal moments of inertia.

9.0 References

1. "Autonomous Momentum Management For Space Station" prepared for the Marshall Space Flight Center, Hunstville, Ala. by Bendix GSD on 15 October 1984

2. Kennel, H. F. "Steering Law for Parallel Mounted Double Gimbal Control Moment Gyros-Revision A", NASA TM-82390 January 1981